Measurement of TPE with electron/positron elastic scattering off the proton

Brian Raue[1,a)]

[1]*Florida International University, Miami, FL, U.S.A. 33199*

[a)]baraue@fiu.edu

Abstract. Three recent experiments have used the ratio of e^+p to e^-p elastic scattering to directly determine the two-photon exchange (TPE) contribution to the elastic-scattering process. These experiments by CLAS, VEPP-3 and OLYMPUS were motivated by the discrepancy between Rosenbluth separation and polarization transfer measurements of the electromagnetic form factors of the proton. The results of these experiments cover $Q^2 < 2$ GeV^2 and collectively agree well with TPE model predictions that largely explain the form factor discrepancy.

INTRODUCTION

The electromagnetic form factors are the fundamental observables that contain information about the spatial distribution of the charge and magnetization inside the proton. The electric ($G_E(Q^2)$) and magnetic ($G_M(Q^2)$) form factors have been extracted by analyzing data from both unpolarized [1, 2, 3, 4, 5, 6] and polarized [7, 8, 9, 10, 11] electron scattering experiments assuming an exchange of a virtual photon between the electron and the proton while accounting for soft radiative effects and external hard photons. The ratio of the electric to magnetic form factors, $\frac{\mu_p G_E(Q^2)}{G_M(Q^2)}$, where μ_p is the proton magnetic moment, extracted from these two experimental methods shows a significant discrepancy that grows with Q^2, as seen in Fig. 1.

One explanation for the observed discrepancy results from neglecting hard two-photon exchange (TPE) corrections [14, 15, 16, 17], a higher-order contribution to the radiative corrections [18, 19, 20]. A model-independent way of measuring the size of the TPE effect is by comparing e^-p and e^+p elastic scattering cross sections [21]. The interference between one- and two-photon exchange diagrams has the opposite sign for electrons and positrons while most of the other radiative corrections are identical for electrons and positrons and cancel to first order in the ratio

$$R = \frac{\sigma(e^+p)}{\sigma(e^-p)}. \tag{1}$$

Correcting for other radiative effects that do not cancel in the ratio, one obtains

$$R_{2\gamma} \approx 1 - 2\delta_{2\gamma}. \tag{2}$$

TPE EXPERIMENTS

In the 1960s and 1970s there were several attempts to measure $R_{2\gamma}$. Early measurements comparing electron and positron elastic-scattering cross sections (see Ref. [21] for a global comparison) were largely limited to low Q^2 and/or high ε, where calculations [22, 23, 24] suggest that TPE contributions are small. Given the limited experimental sensitivity of these early measurements, none of the experiments observed a significant deviation from $R_{2\gamma} = 1$ and the search for TPE effects was dormant. However, the form-factor discrepancy inspired a new round of experiments by the CLAS [25, 13], VEPP-3 [26], and OLYMPUS [27] collaborations. These three experiments used different techniques and each had its own advantages and disadvantages.

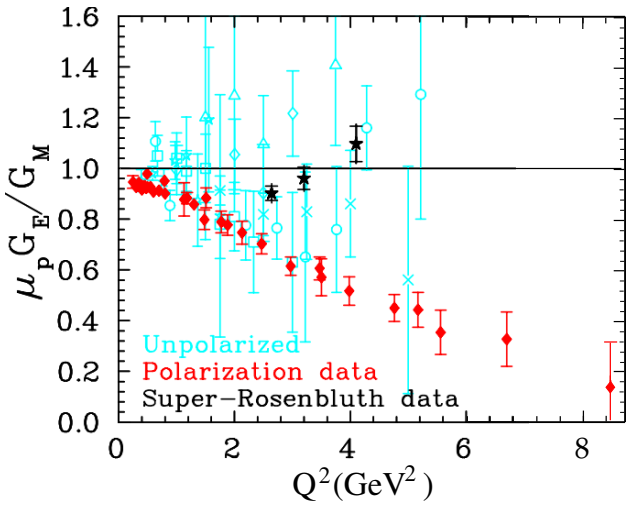

FIGURE 1. Ratio of $\frac{\mu_p G_E(Q^2)}{G_M(Q^2)}$ from Rosenbluth [12] (open cyan symbols) and "Super Rosenbluth" [6] (black stars) measurements and from polarization measurements [7, 8, 9, 10, 11] (filled red diamonds) measurements. Figure adapted from Ref. [13].

The CLAS experiment conducted in Hall B at Jefferson Lab utilized a simultaneous mixed beam of electrons and positrons with a continuous distribution of usable beam energies from 0.85 to 3.5 GeV and the CEBAF Large Acceptance Spectrometer (CLAS) to detect the scattered leptons and protons over a wide range of scattering angles. The mixed beam was produced by a 5.5 GeV primary electron beam incident upon a radiator to produce a secondary photon beam. The photon beam was then incident upon a converter foil that pair-produced the electrons and positrons in the tertiary mixed beam. This conversion process led to large backgrounds in the hall and a large-diameter tertiary beam that together limited the luminosity, which in turn limited the statistical precision of the data. The large acceptance of CLAS led to a wide range of kinematic coverage as shown in Figure 2. By using a simultaneous e^+ e^- beam, there was no need for absolute luminosity normalization in the measured e^+/e^- ratio. A total of 12 independent data points for $R_{2\gamma}$ were measured by CLAS.

The VEPP-3 experiment was conducted on the Novosibirisk storage ring with an internal hydrogen gas target and took data with beam energies of 1.6 and 1.0 GeV during two separate running periods. The experiment used non-magnetic spectrometers, which guarantees identical acceptances for e^+p and e^-p events. This constituted a relative

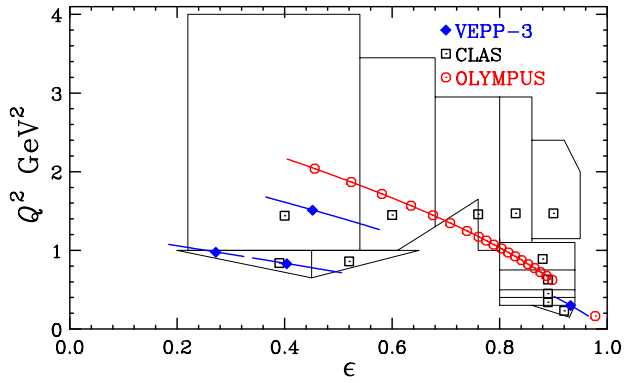

FIGURE 2. Kinematic regions probed by the three two-photon experiments showing the Q^2 and ε plane. Symbols indicate values at which data points were reported by the respective experiments. The boxed regions show the bins over which the CLAS data are summed and the blue curves indicate the kinematic region over which the VEPP-3 data points are summed to obtain the results at the data points shown by the symbols. The binning of the OLYMPUS data are binned such that the gaps between bins are not visible in the red curve. Figure adapted from Ref. [28].

advantage for the VEPP-3 experiment compared to the CLAS and OLYMPUS experiments, which both used magnetic spectrometers and can lead to acceptance differences for the two types of events. The experiment alternated between running with positron and electron beams but did not determine an absolute positron/electron normalizations. Instead, luminosity normalization points were take at small angles where hard TPE effects are expected to be small and $R_{2\gamma} = 1$. This leads to an unknown relative normalization with the measured ratios requiring scaling such that the luminosity normalization points agree with any model predictions. Running with fixed beam energies and fixed spectrometer angles led to high precision results, but at only four kinematic points (see Figure 2).

The OLYMPUS experiment was conducted using the DORIS storage ring at DESY with a 2.01 GeV beam on an internal gas target. Scattered particles were detected with the BLAST detector giving a large coverage of scattering angles from 25° to 75° (see Figure 2). As with the VEPP-3 experiment, the separate electron/positron running required relative normalization. However, unlike VEPP-3, OLYMPUS measured an absolute normalization [29], which was claimed to be good to less than 0.5%. The OLYMPUS experiment resulted in 20 high precision data points.

RESULTS

A direct comparison of all of the results from this new generation of TPE experiments is not straightforward because the data span a large range in both Q^2 and ε. However, comparisons can be made at similar kinematics. Figure 3 shows the ε dependence of the results at $Q^2 = 0.85$ and 1.45 GeV^2 and Figure 4 shows the Q^2 dependence at $\varepsilon = 0.45$ and $\varepsilon = 0.88$. It is clear from the figures that the new results show an marked improvement over the older world data. There is very good agreement between the CLAS and VEPP-3 results but they do not agree well with the OLYMPUS results. CLAS and VEPP-3 results also agree well with the calculations of Zhou and Yang [30] as well as that of Blunden *et al.* [31].

GLOBAL ANALYSIS

In order to better understand the significance of the new results, a global analysis was performed in a recent review article [28]. One way to compare the data is to plot each data point's difference from a given model, $R_{2\gamma}^{\text{data}} - R_{2\gamma}^{\text{model}}$. However, this does not present the entire picture since CLAS and OLYPUS data both have scale-type, or normalization uncertainties that could move the entire data sets up or down.To account for the normalization uncertainty a statistical analysis was preformed in which the CLAS and OLYMPUS data normalization was allowed to float independently but

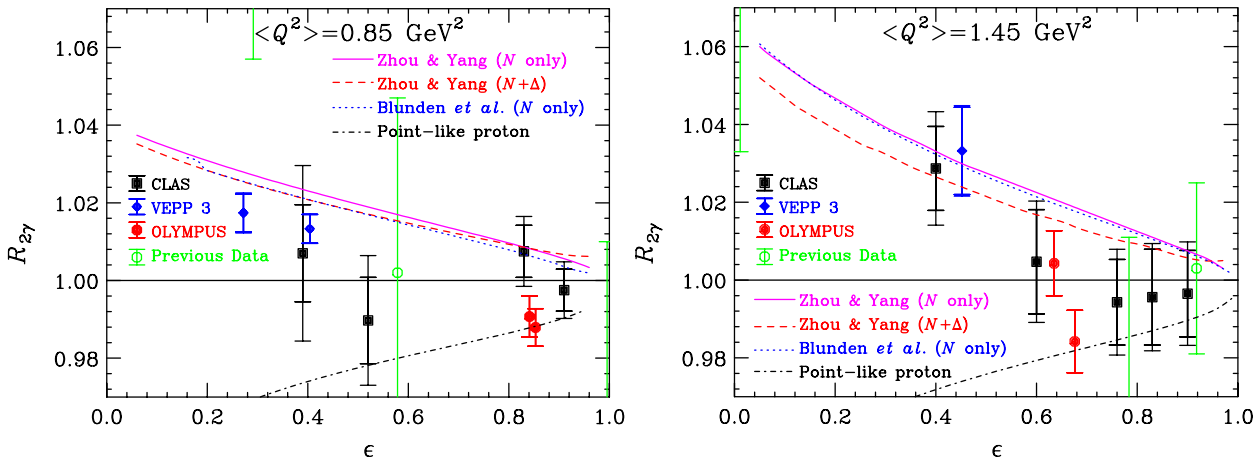

FIGURE 3. World data for $R_{2\gamma}$ at fixed Q^2. The filled black squares are from CLAS [13], the blue diamonds are from VEPP-3 [26], the red circles are from OLYMPUS [27], and the green diamonds are the earlier world data. The line at $R_{2\gamma} = 1$ is the limit of no TPE. The magenta solid and red dashed curves show the calculation by Zhou and Yang [30] including N only and $N + \Delta$ intermediate states, respectively. The blue dotted curve shows the calculation by Blunden *et al.* [31]. The black dot-dashed line shows the calculation of TPE effects on a structureless point proton [20].

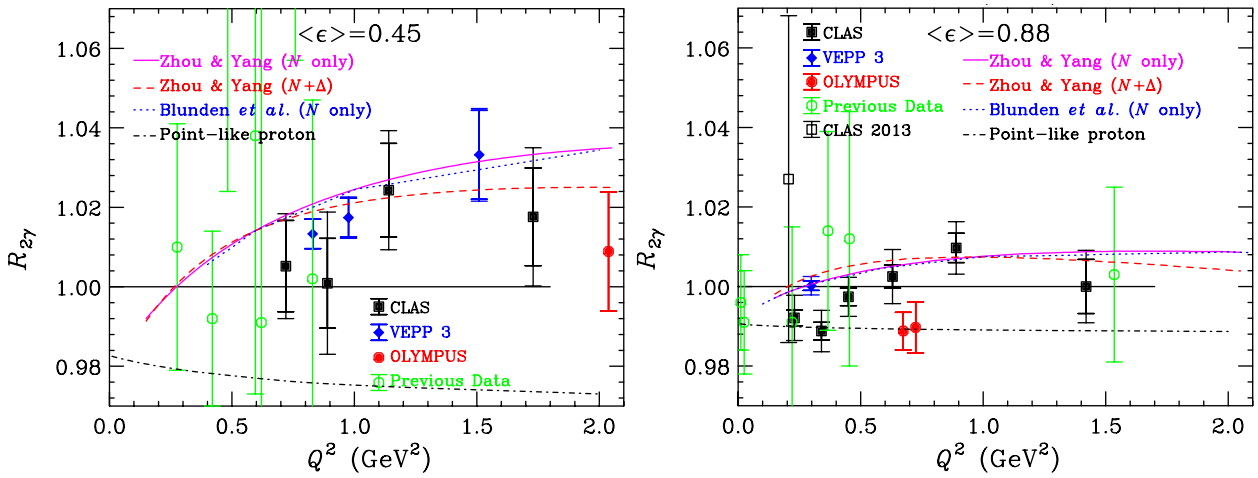

FIGURE 4. World data for $R_{2\gamma}$ at fixed ε. The symbols and curves are the same as in Figure 3 with an additional data point from a CLAS TPE test run [32].

with a penalty determined by the normalization uncertainty. A normalization factor, N, is determined that minimizes a modified χ^2 defined by

$$\chi^2 = \sum_n \left(\frac{R_{2\gamma} N - R_{2\gamma}^{\rm calc}}{\delta R_{2\gamma}^{\rm total}} \right)^2 + \left(\frac{N-1}{\delta R_{2\gamma}^{\rm norm}} \right)^2 , \tag{3}$$

where $R_{2\gamma}$ is the value reported by the experiments, $\delta R_{2\gamma}^{\rm total}$ is the quadrature sum of the statistical and uncorrelated systematic uncertainties, $R_{2\gamma}^{\rm calc}$ is the calculated value for a particular model, and $\delta R_{2\gamma}^{\rm norm}$ is the normalization uncertainty. The number of degrees of freedom, ν, is then number of data points, n, in the set minus one. In total, 34 data points were used for the comparison with two normalization factors leading $\nu = 32$. The analysis for the VEPP-3 data requires a normalization so that the luminosity normalization data point to agrees with the calculation at that point.

For this analysis the comparisons made were to the no-TPE hypothesis ($R_{2\gamma} = 1$) and hadronic model calculations of Blunden and Melnitchouk [33] and by Borisyuk and Kobushkin [34]. The Blunden and Melntichouk calculation determines the TPE correction assuming proton and Δ intermediate states in a dispersive model while the Borisyuk and Kobushkin calculation includes πN intermediate states with $J = 1/2$ and $3/2$. These models largely reconcile the difference between the Rosenbluth and polarization transfer measurements of the form factor ratio.

The difference $R_{2\gamma}^{\rm norm} - R_{2\gamma}^{\rm calc}$ is shown in Figure 5 as a function of ε and the results of the statistical analysis is shown in Table 1. A large difference is clearly seen for the no TPE hypothesis. Statistically, it is excluded at the 99.5% confidence level. There is good agreement with the hadronic models of Reference [33, 34] with confidence levels of 53% and 48%, respectively. However, large upward normalizations are required for the OLYMPUS data that is about a factor of two larger than the normalization uncertainty.

CONCLUSIONS

While the statistical analysis excludes the no TPE hypothesis and seems to indicate a good agreement between the data and leading models, the current state of affairs is by no means definitive. The OLYMPUS data requires a normalization that is about twice as large as the quoted normalization uncertainty. Furthermore, the current data are all below where the form factor discrepancy is significant ($Q^2 > 2$ GeV^2). Clearly, more data at larger Q^2 are needed.

A dedicated positron beam at Jefferson Lab could lead to these much needed data. In addition to Rosenbluth separations using a positron beam in either Hall A or C, one could conduct an OLYMPUS-style experiment with CLAS12. With an 11 GeV beam, the large acceptance ($5^\circ \le \theta_{CM}^e \le 122^\circ$) of CLAS12 could extend measurements of $R_{2\gamma}$ to Q^2 up to ~ 10 GeV^2, and possibly once and for all resolve the form factor discrepancy.

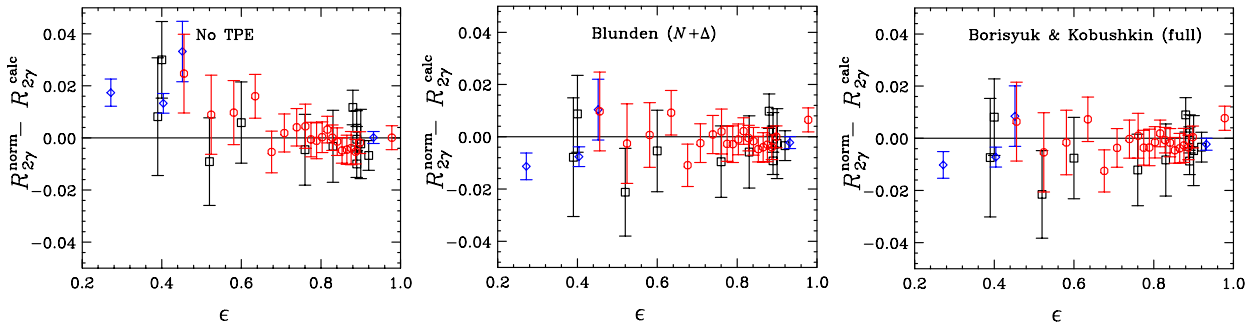

FIGURE 5. Difference between normalized $R_{2\gamma}$ and predictions. Blue diamonds are VEPP-3, black boxes are CLAS, and red circles are OLYMPUS. Figure adapted from Ref. [28].

TABLE 1. Comparison of VEPP-3, CLAS, OLYMPUS, and the combined data set (All) to various TPE calculations showing the reduced χ^2 value and the normalization factor N derived from the fit.

Data set	χ^2_ν	ν	N	$\left(\frac{N-1}{\delta R_{2\gamma}^{\rm norm}}\right)$
Model: $R_{2\gamma} = 1$				
VEPP-3	7.97	4	–	–
CLAS	1.25	11	1.0012	0.40
OLYMPUS	0.68	19	1.0034	0.76
All	1.73	34	–	–
Model: Blunden & Melnitchouk [33]				
VEPP-3	2.62	4	–	–
CLAS	0.91	11	1.0032	1.07
OLYMPUS	0.64	19	1.0082	1.82
All	0.96	34	–	–
Model: Borisyuk & Kobushkin [34]				
VEPP-3	2.28	4	–	–
CLAS	0.94	11	1.0038	1.27
OLYMPUS	0.75	19	1.0097	2.16
All	1.00	34	–	–

ACKNOWLEDGMENTS

This work is supported by the U.S. Department of Energy under grant DE-FG02-99EF41065.

REFERENCES

[1] R. C. Walker *et al.*, Phys. Rev. D **49**, p. 5671 (1994).
[2] L. Andivahis *et al.*, Phys. Rev. D **50**, p. 5491 (1994).
[3] C. Berger, V. Burkert, G. Knop, B. Langenbeck, and K. Rith, Phys. Lett. B **35**, p. 87 (1971).
[4] J. Litt *et al.*, Phys. Lett. B **31**, p. 40 (1970).
[5] M. E. Christy *et al.*, Phys. Rev. C **70**, p. 015206 (2004).
[6] I. A. Qattan *et al.*, Phys. Rev. Lett. **94**, p. 142301 (2005).
[7] V. Punjabi *et al.*, Phys. Rev. C **71**, p. 055202 (2005).
[8] A. J. R. Puckett *et al.*, Phys. Rev. Lett. **104**, p. 242301 (2010).
[9] A. J. R. Puckett *et al.*, Phys. Rev. C **85**, p. 045203 (2012).
[10] X. Zhan *et al.*, Phys. Lett. **B705**, 59–64 (2011).

[11] G. Ron *et al.*, Phys. Rev. C **84**, p. 055204 (2011).
[12] J. Arrington, Phys. Rev. C **68**, p. 034325 (2003).
[13] D. Rimal *et al.* (CLAS), Phys. Rev. **C95**, p. 065201 (2017).
[14] P. A. M. Guichon and M. Vanderhaeghen, Phys. Rev. Lett. **91**, p. 142303 (2003).
[15] P. G. Blunden, W. Melnitchouk, and J. A. Tjon, Phys. Rev. Lett. **91**, p. 142304 (2003).
[16] Y. C. Chen, A. Afanasev, S. J. Brodsky, C. E. Carlson, and M. Vanderhaeghen, Phys. Rev. Lett. **93**, p. 122301 (2004).
[17] J. Arrington, Phys. Rev. **C69**, p. 022201 (2004).
[18] J. Arrington, W. Melnitchouk, and J. A. Tjon, Phys. Rev. C **76**, p. 035205 (2007).
[19] C. E. Carlson and M. Vanderhaeghen, Ann. Rev. Nucl. Part. Sci. **57**, p. 171 (2007).
[20] J. Arrington, P. Blunden, and W. Melnitchouk, Prog. Part. Nucl. Phys. **66**, 782–833 (2011).
[21] J. Arrington, Phys. Rev. C **69**, p. 032201 (2004).
[22] S. D. Drell and M. Ruderman, Phys. Rev. **106**, p. 561 (1957).
[23] S. D. Drell and S. Fubini, Phys. Rev. **113**, p. 741 (1959).
[24] G. K. Greenhut, Phys. Rev. **184**, p. 1860 (1969).
[25] D. Adikaram *et al.* (CLAS), Phys. Rev. Lett. **114**, p. 062003 (2015).
[26] I. A. Rachek *et al.*, Phys. Rev. Lett. **114**, p. 062005 (2015).
[27] B. S. Henderson *et al.* (OLYMPUS), Phys. Rev. Lett. **118**, p. 092501 (2017).
[28] A. Afanasev, P. G. Blunden, D. Hasell, and B. A. Raue, Prog. Part. Nucl. Phys. **95**, 245–278 (2017).
[29] A. Schmidt, C. O'Connor, J. C. Bernauer, and R. Milner, Nucl. Instrum. Meth. **A877**, 112–117 (2018).
[30] H.-Q. Zhou and S. N. Yang, Eur. Phys. J. **A51**, p. 105 (2015).
[31] P. G. Blunden, W. Melnitchouk, and J. A. Tjon, Phys. Rev. C **72**, p. 034612 (2005).
[32] M. Moteabbed *et al.*, Phys. Rev. C **88**, p. 025210 (2013).
[33] P. G. Blunden and W. Melnitchouk, Phys. Rev. **C95**, p. 065209 (2017).
[34] D. Borisyuk and A. Kobushkin, Phys. Rev. **C92**, p. 035204 (2015).